

Oscillatory motion and merging responses of primary and satellite droplets from Newtonian liquid jets

VISWANATHAN, Harish

Available from Sheffield Hallam University Research Archive (SHURA) at:

<https://shura.shu.ac.uk/25400/>

This document is the Accepted Version [AM]

Citation:

VISWANATHAN, Harish (2019). Oscillatory motion and merging responses of primary and satellite droplets from Newtonian liquid jets. *Chemical Engineering Science*, 212, p. 115334. [Article]

Copyright and re-use policy

See <http://shura.shu.ac.uk/information.html>

Oscillatory Motion and Merging Responses of Primary and Satellite Droplets from Newtonian Liquid Jets

H. Viswanathan*

Department of Engineering and Mathematics, Sheffield Hallam University, Howard Street, Sheffield, England, S1 1WB, United Kingdom

ABSTRACT

Numerical simulations of laminar Newtonian liquid jets are presented that divulge several breakup and merging responses for both primary and satellite droplets. Using an axisymmetric VOF model, we predict the presence of surface oscillations of droplets disintegrated from jets, which at times lead to merging of droplets when travelling downstream. Our simulations indicate that when primary droplets undergo merging, they exhibit characteristics such as *i*) permanent and *ii*) partial coalescence. We find that the partial coalescence of droplets can lead to a *reflexive-like* separation and then show *re-merge* responses. The formation of an air-bubble during the merging of binary droplets is predicted. Characteristics such as forward, rear, and simultaneous merging patterns of satellites with primary droplets are captured in our numerical simulations. Furthermore, a new merging pattern is reported wherein, satellites formed from the swellings of the jet can be absorbed back into the moving core of the liquid jet.

Keywords: Liquid Jet; VOF; Coalescence of drops; Air-Entrapment; Merging of Satellite drops; Reflexive-Like Separation.

Highlights

- Axisymmetric VOF simulations are performed which predict surface oscillations in droplets that are disintegrated from a Newtonian liquid jet which aid (i) permanent coalescence and (ii) partial coalescence leading to a *reflexive-like* separation.
- The *reflexive-like* separation shows *re-merging* of droplets when they move downstream owing to the presence of undamped surface oscillations.
- Forward merge, rear merge and simultaneous merging of satellite droplets are predicted in liquid jets that have been observed in previously published experimental results.
- A new mode of satellite merging is predicted where the disintegrated satellite is absorbed back into the moving jet liquid core.
- The formation of air-entrapment is numerically detailed during coalescence events.

1. Introduction

In many applications such as, but not restricted to ink-jet printing, encapsulation, food engineering and chemical synthesis, the fundamental implications of drop formation from liquid jets become indispensable. In such applications, liquid jets tend to produce satellite drops which are interposed amongst the primary droplets owing to various parameters. Some parameters in the liquid jet, such as the effect of perturbations, growth rates, and breakup times influence the breakup and merging of primary drops. Also, however, the merging behaviour of droplets is influenced by the surface oscillation of droplets when moving downstream. Several eminent researchers in the past have investigated the breakup of drops from liquid jets (Savart, 1833; Plateau, 1873; Rayleigh, 1878) using both experiments and linear stability analysis. Rayleigh (1882) further presented a dispersion equation that relates to the temporal instability of the jet as a function of wavenumber. Rayleigh's analysis was extended by Tomotika (1935) that showed that the instability of the liquid jet was strongly influenced by the ratios of the viscosity and densities of the jet and Ohnesorge number. However, given the nature of the nonlinearities and complexities involved with a jet breakup led to further theoretical developments by including finite-amplitude surface disturbances by incorporating third-order effects in describing a jet (Yuen, (1968); Nayfeh, (1970)). Goedde and Yuen (1970) measured the nonlinear variation of the pressure distribution between the drop pressure and the ligament pressure and compared them with the analytical solution for capillary instability for a viscous jet developed by Chandrasekhar (1961). Further investigations by Rutland and Jameson (1970) led to a deeper understanding of the nonlinear behaviour of capillary jet where, it was shown that in a synchronized breakup of the jet, smaller satellite droplets are formed that are sometimes interspaced between the main 'primary' droplets and can consequently merge (Pimbley and Lee, (1977); Chaudhary and Maxworthy, (1980)). Experimental investigations by Vassallo and Ashgriz, (1991) revealed that the satellites that formed during a jet breakup exhibit distinctive breakup patterns such as forward merging, rear merging and reflexive merging depending on the type of jet wavelengths and disturbance amplitudes. Besides, size ratios of the satellite to primary drops and their corresponding breakup times were revealed in their experiments. The merging behaviour of the droplet breakup from liquid jets has been

significantly investigated more recently by Driessen et al. (2014) who showed that in a controlled breakup by super-positioning of two Rayleigh-Plateau unstable modes, droplets that disintegrate from liquid jets due to different velocities eventually coalesce and form larger droplets spaced at a much larger distance than the initial droplets. Conversely, for the case of a free or during a random breakup of droplets from Rayleigh jetting regime, the coalescence of drops was shown to widely be promoted by the oscillation of droplets after the breakup. Also, it was reported that even if the distance between droplets is kept constant, the amplitude of the oscillation was found to be sufficiently large to allow droplets to collide and, consequently, bounce or coalesce (Suñol and Cinca, 2015).

From a numerical perspective, during the past two decades, several one-dimensional (1D) models have been proposed to describe the behaviour of capillary jets through a global stability analysis (Leib and Goldstein, (1986); Eggers and Dupont, (1994); Garcia and Castellanos, (1998)). However, the global stability analysis is greatly simplified owing to the slender jet approximation, and experimentally the jet is stable at lower flow rates than compared to the predictions from the global stability analysis (Sauter and Buggisch, (2005)). With recent advancements in (1D) modelling through the use of Differential-Algebraic equations (DAE) and by incorporating both the linear stability analysis and the nonlinear transient behaviour, it was possible to obtain equilibrium solutions for capturing slender jets and examine the dripping to jetting transitions (Rodríguez and Saborid, (2017)). However, with the limitations and the problems associated with both the perturbation analysis and the one-dimensional depictions in predicting the dynamics of jet breakup especially in detailing the downstream events, it is of great interest to solve the full Navier-Stokes equations numerically.

Three dimensional (3D) numerical simulations for laminar jetting have been carried out by various authors, using Level Set Method (LSM) (Pan and Suga, (2006)), using a Volume of Fluid Method (Delteil et al., (2011)), and with Coupled Level Set Volume of Fluid (CLSVOF) methods (Xiao et al., (2016)) by integrating the Continuum Surface Force (CSF) approach which have shown to robustly capture the Rayleigh droplet breakup. More recently, the axisymmetric models using CLSVOF (Chakraborty et al., 2016; Borthakur et al., 2017) and VOF (Viswanathan, (2019)) have numerically explored the transition from dripping to jetting and to predict the breakup regimes adequately. Viswanathan (2019) presented numerical simulations

for periodic dripping, dripping faucet and transition modes that lead to jetting and validated with experimental results obtained by Clanet and Lashreas (1999). Also, the simulations from Viswanathan (2019) showed different responses that characterize the dripping and the dripping faucet regimes leading to chaotic dripping patterns. Within the chaotic regime, four unique modes of satellite formation and their merging patterns were reported. Detailed temporal variations within the jetting regime were presented alongside its dependence on Weber Number (We) by comparing the numerical predictions of the mean jet breakup length and experimental correlations derived by Sallam et al. (2002). More importantly, the work of Viswanathan (2019) elucidated the downstream behaviour of drops after jet disintegration, wherein the oscillatory motion of drops and coalescence patterns were predicted. Through various spatial and temporal resolutions, it was explicated that of the many complex dynamics that influence the primary droplet coalescence, the oscillatory motion of drops during their travel downstream, which is dampened usually due to viscous effects, can be influential in aiding to a collision of two droplets which may finally coalesce.

Head-on and off-centre collision outcomes of binary droplets themselves have shown to exhibit complex physics such as coalescence, stretching separation, reflexive separation and bouncing, which have been demonstrated experimentally by several researchers over the last few decades (Brazier-Smith et al., (1979); Ashgriz and Poo, (1992); Qian and Law, (1997); Orme, (1997)). Subsequently, numerical simulations (Mashayek et al. (2003); Pan and Suga, (2005)) to binary collision outcomes that substantiated the experimental counterparts through methods such as VOF (Nikolopoulos and Bergeles, (2011)) and through Lattice-Boltzmann techniques (Premnath and Abraham, (2005) aided to a more profound understanding of the merging behaviour of binary droplets alongside predictive modelling approaches (Munnannur and Reitz, (2007); Krishnan and Loth, (2015)).

In this study, however, we will direct our attention to droplets that are disintegrated from a laminar Newtonian liquid jet, that undergo oscillatory motion when travelling downstream and their influence on merging behaviour. The motivation for the present work is derived from experimental findings of Vassallo and Ashgriz (1991), Pimbley and Lee (1977) for generic droplet merging behaviour that is observed for liquid jets and generic features of binary collisions observed by several researchers (Brazier-Smith et al., (1979); Ashgriz and Poo, (1992); Qian and Law,

(1997); Orme, (1997)). Numerically, however, several questions remain unanswered for droplets that are disintegrated from a liquid jet and undergo surface oscillations; such as *a) what merging patterns do primary drops experience during their downward motion? b) For regimes that show satellite drop formation, how does a satellite drop interact or even merge with the primary drop, during its downstream travel when emanated from a Rayleigh Jet?* Also, to test the capability of VOF model in predicting the merging patterns that have been reported in the previous experimental observations, this paper shall focus on numerically examining the downstream behaviour, and their merging patterns of both primary and satellite drops devising from the previously validated numerical model of Viswanathan (2019).

2. Numerical Model for Liquid Jet Breakup

An axisymmetric domain represented in Fig. 1 is chosen for the present study where water at constant flow rate Q is injected into still air from a nozzle of diameter D . Both the fluids are treated as incompressible and Newtonian with a constant water-air interface surface tension σ .

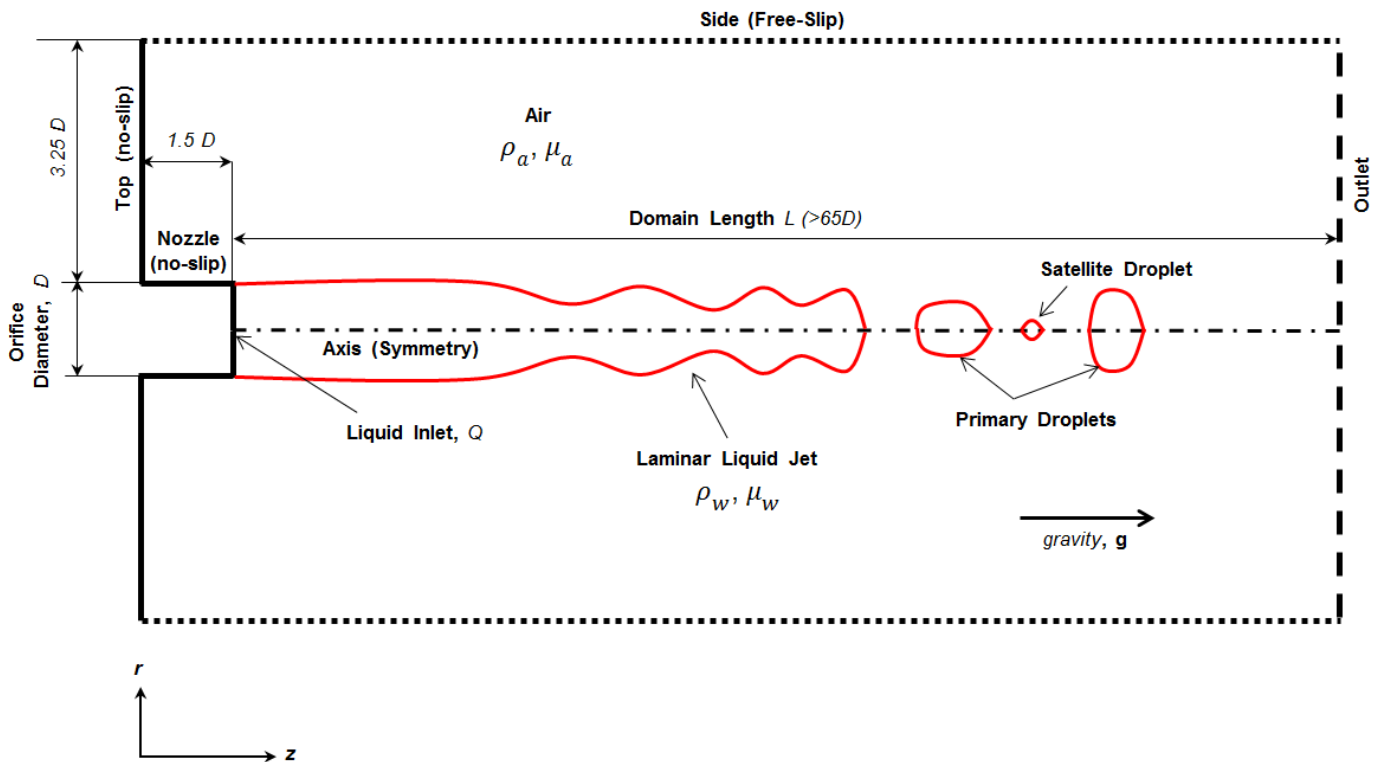


Fig.1. Schematic of an axisymmetric domain showing boundary conditions, computational domain size used for modelling laminar liquid jet breakup.

The density and viscosity are expressed as ρ_w, ρ_a and μ_w, μ_a for the phases namely, water and air respectively. The present treatment of axisymmetric approach to understanding the jet breakup has been investigated by several researchers (Chakraborty et al., 2016; Moallemi et al., 2016; Xie et al., 2017; Borthakur et al., 2017) and more recently by Viswanathan (2019) using various different interface capturing techniques.

In the present study, the equations of motion that best describe this system are modelled using a single set of two-dimensional, incompressible, axisymmetric

Navier-Stokes Equations coupled with VOF method which define the interface between immiscible fluids, namely, water and quiescent air and providing volume fraction conservation throughout the domain. The governing equations for mass and momentum balance are given as follows:

$$\frac{\partial \rho}{\partial t} + \frac{\partial(\rho V_i)}{\partial X_i} = 0 \quad (1)$$

$$\frac{\partial(\rho V_i)}{\partial t} + \frac{\partial(\rho V_i V_j)}{\partial X_j} = -\frac{\partial(P)}{\partial X_i} + \frac{\partial}{\partial X_j} \mu \left(\frac{\partial V_i}{\partial X_j} + \frac{\partial V_j}{\partial X_i} \right) + \rho g_i + F_i \quad (2)$$

In the above equation, P is the pressure, V_i, V_j correspond to the components of the velocity field, g_i is the acceleration due to gravity and t is the time. F_i is the continuum surface tension force on the interface of the volume fraction field α , given by

$$F_i = \sigma k \nabla \alpha \quad (3)$$

where k is the local curvature on the interface and is computed as

$$k = -\nabla \cdot \left(\frac{\nabla \alpha}{|\nabla \alpha|} \right) \quad (4)$$

For describing the interface between immiscible fluids, namely, water and quiescent air and providing volume fraction conservation throughout the domain, two-phase flow using the VOF equation by Hirt and Nichols (1981) is employed as follows:

$$\frac{\partial \rho}{\partial t} + \frac{\partial(V_i \alpha)}{\partial X_i} = 0 \quad (5)$$

The volume fraction gives the portion of the cell which is filled with either phase, where

$\alpha = 0$ the cell is filled with air (the continuous fluid)

$0 < \alpha < 1$ the interface exists in the cell (6)

$\alpha = 1$ the cell is filled with liquid (the dispersed fluid, namely, water in this study)

The density ρ and viscosity μ can be expressed as linear contributions from each phase as follows:

$$\rho = \rho_w \alpha + \rho_a (1 - \alpha) \quad (7)$$

$$\mu = \mu_w \alpha + \mu_a (1 - \alpha) \quad (8)$$

The capillary length scale and the corresponding time scale pertinent to this study are defined as follows:

$$\lambda_c = \sqrt{\frac{\sigma}{(\rho_w g)}} \quad (9)$$

$$t_c = \sqrt{\frac{(\rho_w D^3)}{\sigma}} \quad (10)$$

The current study is limited to laminar jets where the Reynolds number (Re) is given by $Re = \frac{\rho_w V_0 D}{\mu} < 2300$. The other crucial dimensionless number for this study is the Weber number (We) which relates the inertia of the fluid compared its surface tension and illustrates whether the kinetic energy or the surface tension energy is dominant, given by $We = \frac{\rho_w V_0^2 D}{\sigma}$. In the above expressions for Re and We , V_0 is the mean velocity at the nozzle inlet shown in [Fig. 1](#) and is related to the volumetric flow rate, given by $Q = \pi D^2 V_0$. To represent the jetting regime, a domain of length $>65D$ and width $3.75D$ was chosen to resolve the events of interest downstream. The domain was initialized with still air with properties at standard temperature and pressure conditions. A uniform mesh with a dimensionless grid size of $\Delta r^* = \Delta z^* = 0.02$ scaled by D is selected. The selected grid size corresponds to ~ 110 orders of magnitude higher in resolution than compared to the capillary length scale (λ_c) to jet diameter (D) ratio. The resulting total grid corresponds to ~ 2.2 million elements and satisfies the sizing requirements of the grid independency study that was ascertained from previously published work ([Viswanathan, 2019](#)). To reduce the computational resource requirements, only half of the jets were simulated by applying conditions of symmetry along with other boundary conditions for numerical closure, as shown in

Fig. 1. A summary of all parameters that are used in the current study is presented in **Table 1.**

| Description | Values |
|--|-----------------------------|
| <i>Orifice Inlet Diameter (D)</i> | 1.2×10^{-3} mm |
| <i>Domain Length (L)</i> | $>65D$ |
| <i>Domain Width (W)</i> | $3.75 D$ |
| <i>Density of Water (ρ_w)</i> | 1000 kg/m ³ |
| <i>Density of Air (ρ_a)</i> | 1.22 kg/m ³ |
| <i>Viscosity of Water (μ_w)</i> | 10^{-3} Pa s |
| <i>Viscosity of Air (μ_a)</i> | 1.786×10^{-5} Pa s |
| <i>Air-Water Interfacial surface tension (σ)</i> | 0.0728 (N/m) |
| <i>Weber number (We) ranges</i> | 6.62, 10.92, 16.48 |
| <i>Reynolds number (Re) ranges</i> | 760.8, 976.8, 1200 |

Table.1. List of parameters values used in the present study.

The present work was developed using a commercial package ANSYS Fluent (Version 18.0) in an explicit formulation with a maximum Courant number of 0.25, solved using the Non-Iterative Time Advancement (NITA) scheme. The pressure-velocity scheme (PISO) that splits the solution into predictor-corrector steps was used in conjunction with the QUICK scheme to discretize the momentum equation. The VOF equation was discretized using the Geo-Reconstruct (Youngs, 1982) scheme that uses a piecewise-linear approach to determine the interface between fluids. The scalar gradients were computed by the Least-Square Cell-based method. The interfacial forces were accounted for using the Continuum Surface Force (CSF) (Brackbill et al., 1992) such that the addition of surface tension to the VOF calculation results in a source term in the momentum equation. For all residual values, the convergence tolerance achieved within each time-step when monitored was found to be $<10^{-6}$. The aforementioned simulation strategy is consistent with the previously published results from Viswanathan (2019). However, in this paper, we will expand on the work of Viswanathan (2019) for describing the liquid jet disintegration and downstream dynamics for illustrating various merging patterns of both primary and satellite droplets.

3 Results

In this section, we shall present the numerical results for a random breakup of laminar liquid jets for resolving both the spatial and temporal events. In doing so, we shall verify the rationality of our simulations using theoretical descriptions before examining the rich dynamics that evolve downstream during the disintegration of laminar Rayleigh jets.

3.1 Model Verification

In a previous evaluation by Viswanathan (2019), a rigorous study on mesh independency, model validation with experimental data for both dripping and transition to jetting (Clanet and Lashreas, (1999)) and breakup lengths for a fully transitioned Rayleigh liquid jet (Sallam et al., (2002)) has been presented. The reader is directed to the work of Viswanathan (2019) from a model-experimentation validation viewpoint. However, to further verify and to underpin that the capillary effects within the numerical simulation are without parasitic currents, a pressure jump between the outside air and disintegrated liquid droplets emanating from the liquid jet from the numerical simulation in the linear Rayleigh limit is tested using the Young–Laplace’s equation (Delteil et al., (2011)) as follows:

$$\Delta P = \sigma \left(\frac{1}{R_1} + \frac{1}{R_2} \right) \quad (11)$$

where ΔP is the pressure difference across the air-water interface, R_1 and R_2 correspond to the principal radii of curvature in the characteristic planes of the local interface. In the present case, we illustrate using Fig. 2 that shows the relative pressure between air and a water jet that disintegrates into several droplets.

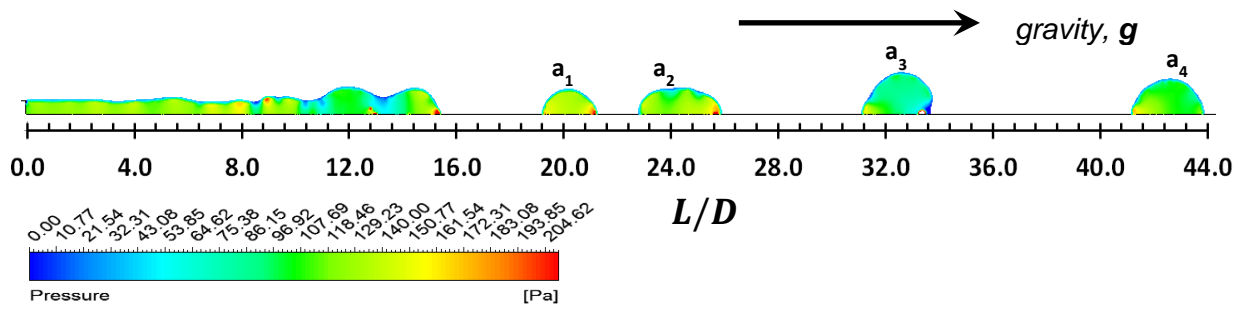


Fig.2. Pressure distribution on the Laminar Water jet with $We=6.62$ injected into still Air.

Considering that $R_1 = R_2$, a comparison of the pressure difference that is obtained from simulation results for the droplets and Young-Laplace equation is presented in [Table 2](#), which suggests a good overall agreement between them.

| Droplets (Fig. 2) | Drop Radius from Simulation (mm) | ΔP_{Theory} (Eq. 11) (Pa) | $\Delta P_{Simulation}$ (Pa) | Relative Error (%) |
|---|---|---|---------------------------------|---------------------------|
| a₁ | 1.258 | 115.739 | 120.212 | 3.864 |
| a₂ | 1.728 | 84.254 | 89.454 | 6.171 |
| a₃ | 1.440 | 101.090 | 93.54 | 7.468 |
| a₄ | 1.595 | 91.242 | 96.333 | 5.579 |

Table.2. Comparison of Pressure Differences across Air-Water interface predicted by Young-Laplace Equation ([Eq.11](#)) against Simulation Results for various drop sizes disintegrated from a Jet with $We=6.62$, as shown in [Fig. 2](#).

3.2 Merging Behaviour of Primary droplets

Droplets that disintegrate from a laminar Newtonian jet undergo surface oscillations that result in prolate-oblate shape patterns when travelling downstream. A schematic of prolate and oblate definitions used in the present work are shown in [Fig. 3](#).

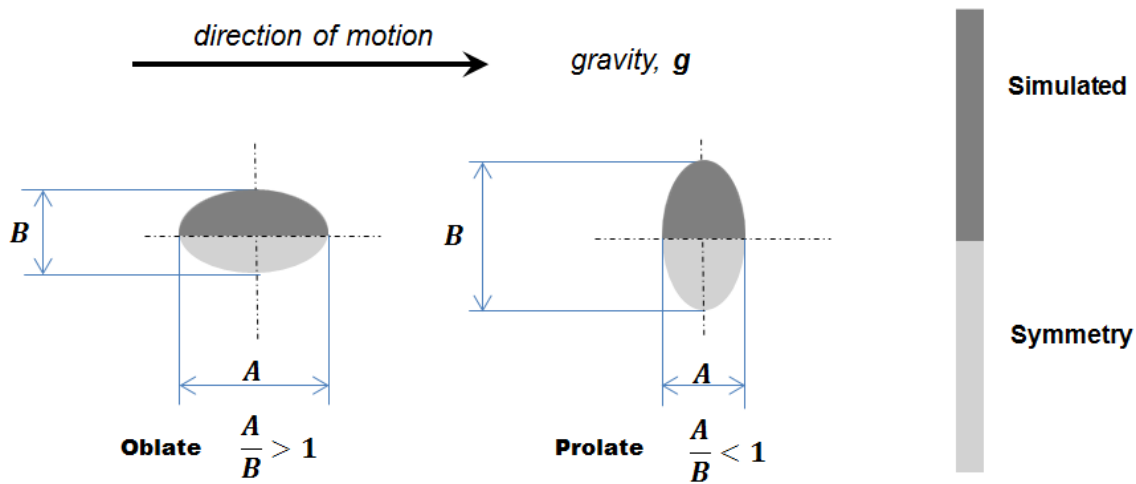


Fig.3. A schematic representation of a drop exhibiting oblate and prolate transformations when moving downstream. A and B represent the diameter of the drop in radial and axial directions, respectively. The dark grey region represents the simulated portion of the droplet, whereas the light grey portion of the droplet represents symmetry.

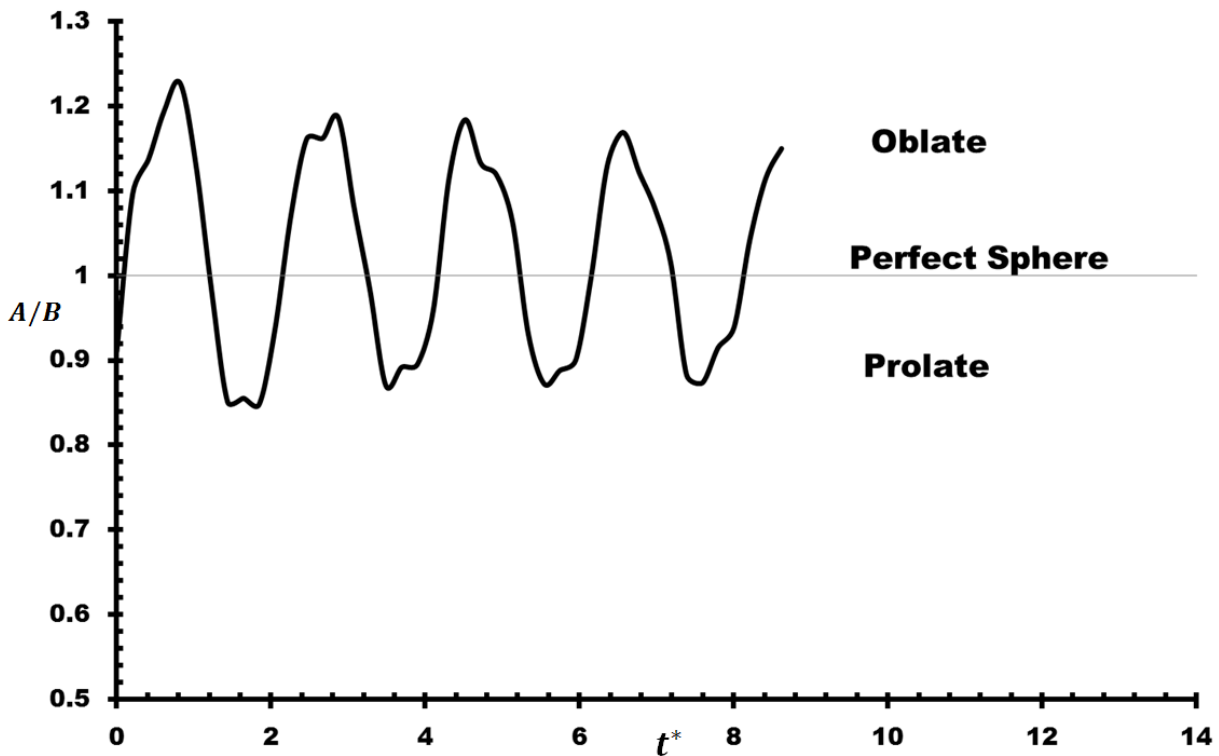


Fig.4. Oscillatory motion of a single drop disintegrated from a Laminar Jet with $We=10.92$.

Fig. 4 shows the surface oscillations of a single droplet moving downstream formed from a laminar jet of $We=10.92$ obtained from present numerical simulations. It can be seen that an initially prolate drop that is disintegrated from the jet transforms into oblate shape via the spherical shape ($A=B$) during its downstream motion over time (t^*); where the dimensionless time $t^* = (t - t_0)/t_c$ and t_0 correspond to the time of formation of the droplet. With each recovery to a perfect sphere through oblate to prolate motion and vice-versa, the presence of highly nonlinear surface oscillations on the droplet are evidenced in the numerical results which are primarily due to the competing inertia and surface tension forces and are eventually dampened by viscous effects over time as observed in experiments (Becker et al., 1991). However, a continuous disintegration of drops from a laminar jet that is composed of several wavelengths would then mean that the droplets are formed with various initial shapes owing to several parameters such as but not restricted to variation in breakup length, jet growth rate and so forth.

Factors such as variations in the initially formed droplet shapes, their degree of nonlinearity, and damping of surface oscillations at different stages when moving downstream influence the collision of droplets with one or more of them that are present downstream. One such case is illustrated in **Fig. 5(a)** where two droplets \mathbf{a}_1 and \mathbf{a}_2 that are formed sequentially from the jet and undergoing very different nonlinear surface oscillations while moving downstream. As seen, \mathbf{a}_1 is formed as an oblate drop, whereas \mathbf{a}_2 is formed as a prolate drop. However, after undergoing over a cycle of surface oscillation to becoming a perfect sphere, the drop \mathbf{a}_1 experiences a rear collision from \mathbf{a}_2 and permanently coalesce to form \mathbf{a}_{12} . Although, intuitively, \mathbf{a}_{12} is formed as an oblate drop owing to both \mathbf{a}_1 and \mathbf{a}_2 exhibiting oblate shapes during the incipience of merging, \mathbf{a}_{12} experiences enhanced surface oscillations than compared to its predecessors which eventually dampen during its motion downstream. Within the scope of our simulations, with over 50 coalescence events observed for each We numbers presented, we observe that the event of a binary collision was always characterized by at least one participating drop exhibiting an oblate shape at the incipience of contact. **Fig. 5(b)** shows the volume fraction profiles of the liquid that correspond to the sequence of events observed in **Fig. 5(a)**. We observe that the drops have coalesced at $t^*= 4.7208$ and interestingly, the presence of air-entrapment is evidenced in the form of a micro-bubble within the coalesced

drop \mathbf{a}_{12} . Such entrapment of air is always observed whenever two droplets coalesced in all our simulations that are reported in the present work and is evidenced in an earlier publication (Viswanathan, (2019)) as well.

Experimental work related to the formation of air bubbles during the merging of two droplets of various size ratios has previously been extensively reported by Ashgriz and Poo (1990) from the context of droplets approaching each other with situations concerning head-on collisions and several off-centre collisions. Numerically, details on entrapment owing to droplet collisions have been comprehensively highlighted by Premnath and Abraham (2005) using Lattice-Boltzmann techniques and Nikolopoulos and Bergeles (2011) using VOF methods for situations detailed by Ashgriz and Poo (1990). In the present numerical work, however, we highlight the formation of an air bubble due to the coalescence of droplets in the same direction of motion and with surface oscillations, i.e., when moving downstream after disintegrating from a laminar liquid jet. A closer examination of one such event of merging is detailed in Fig.6 wherein, a prolate drop \mathbf{a}_2 and an oblate drop \mathbf{a}_1 that is disintegrated sequentially from the liquid jet are shown to merge downstream to form \mathbf{a}_{12} . In each of the part figures a), b) and c) within Fig.6, we show the (i) volume fraction, (ii) shear stress distribution and (iii) instantaneous velocity along the axis normalized by the mean velocity at the inlet V_0 . In this case, the value $t^* = 0$ represents the dimensionless time during the initiation of contact, whereas the $-^{ve}$ and $+^{ve}$ signs associated with t^* indicate the pre and post-collision events. During the pre-collision event shown in Fig.6a, the (ii) shear stress distribution over the interface is relatively high, which is developed during the drop pinch-off from the jet, and owing to surface oscillations experienced by the drop during its downstream motion is detailed. When a contact is initiated between the droplets ($t^* = 0$) shown in Fig.6b, the contact region experiences the highest level of (ii) shear stress distribution within the two droplet masses that are in the process of merging. Fig.6c shows a sharp change in the (iii) velocity profile tending to values closer to zero on the interface curvature between the entrapped air and the droplet is observed suggesting the formation of an air bubble at $t^* = 0.2052$ which corresponds to a physical timestamp of ~ 0.001 s. The merging is thus complete with a formation of a single droplet \mathbf{a}_{12} , with no further breakup observed, within which an air bubble occupying a volume of $\sim 4\%$ in reference to \mathbf{a}_{12} is held. Here, we emphasise that due

to an extremely fine mesh and time-steps involved in the simulation, the air entrainment is well represented.

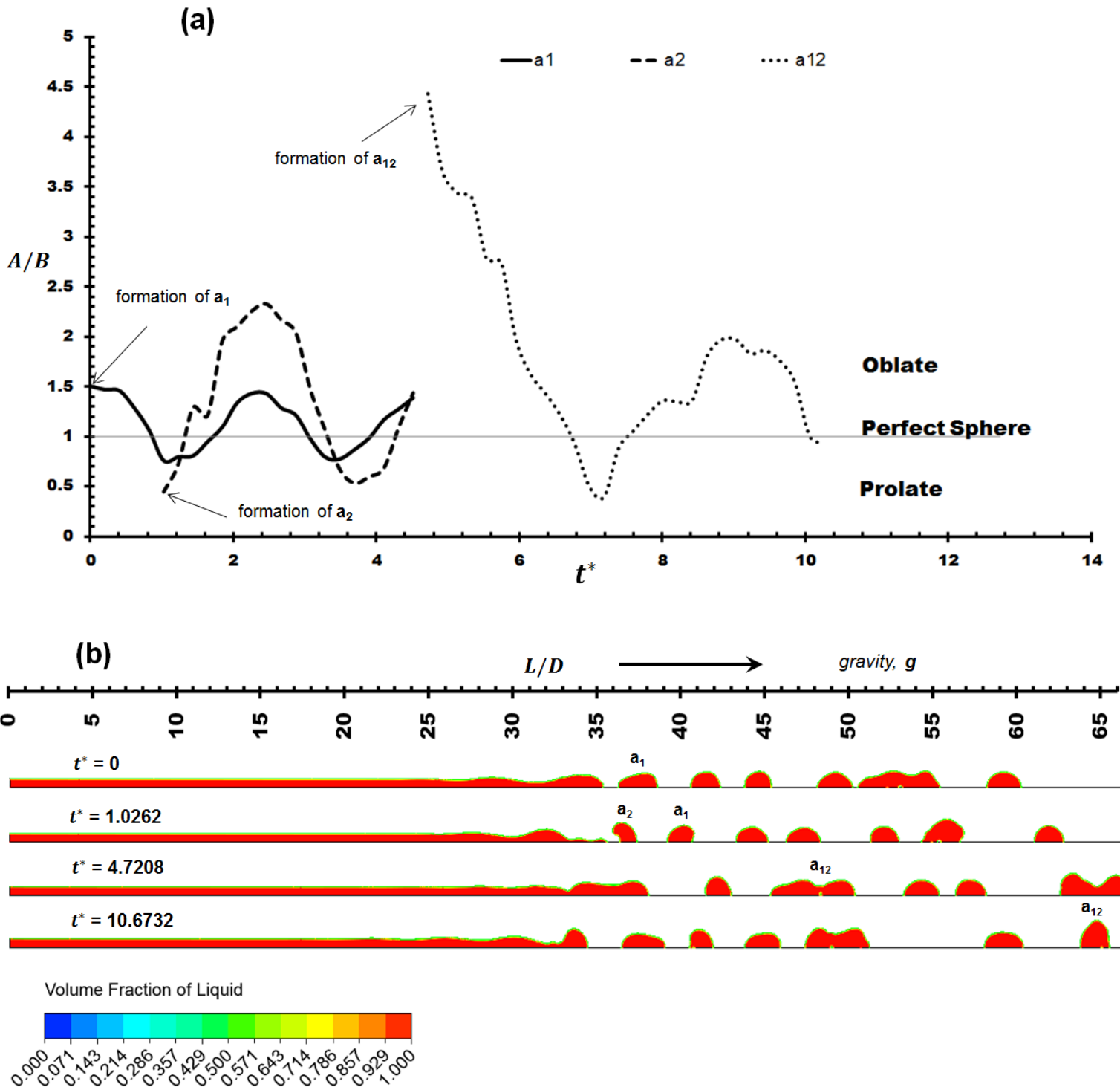


Fig.5. Permanent coalescence of two primary droplets a_1 and a_2 leading to the formation of a drop a_{12} from a Laminar Jet with $We=10.92$. **(a)** Shows the surface oscillations of drops and **(b)** presents the VOF profiles of the droplets and merging event downstream.

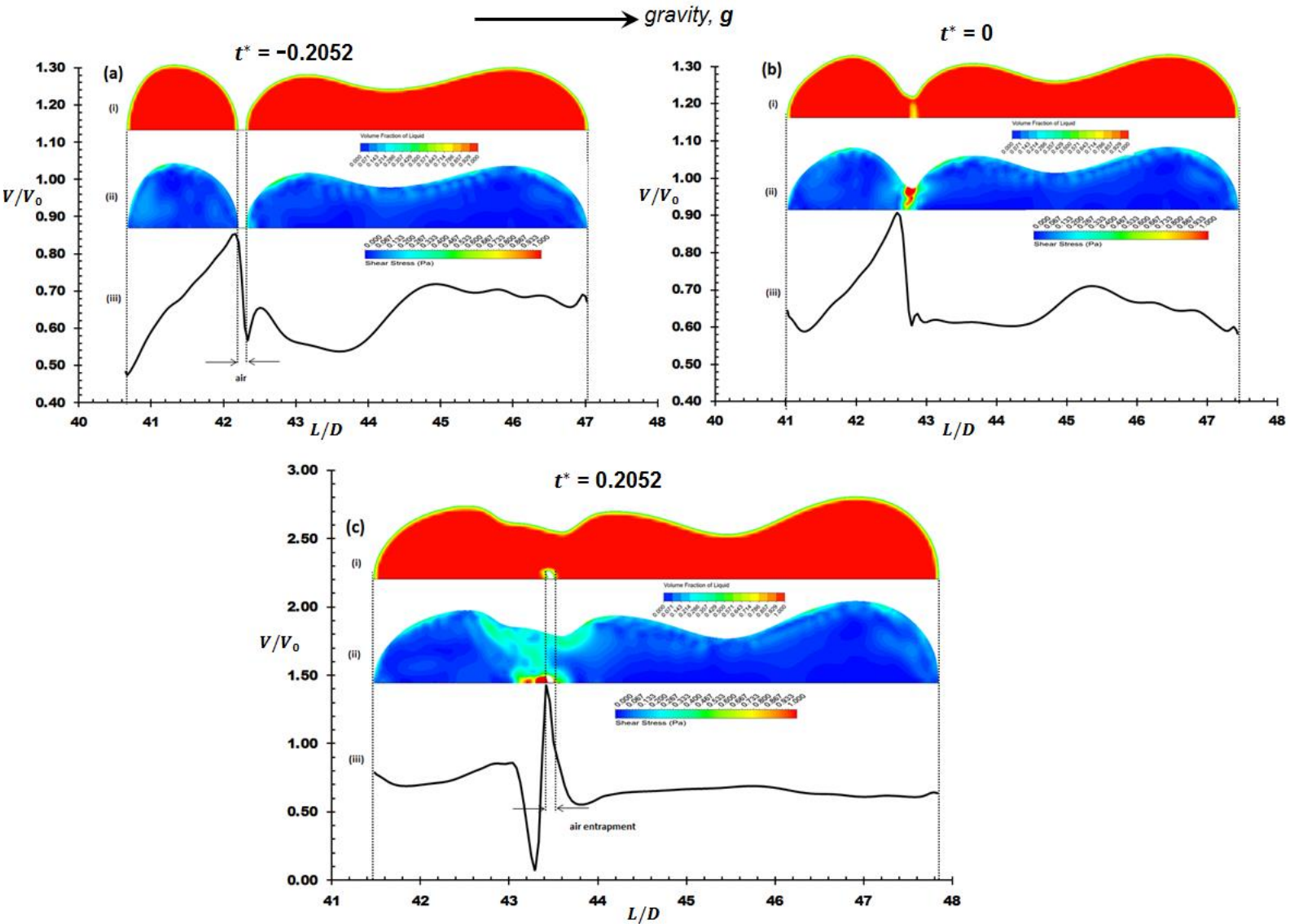


Fig.6. Merging of two primary droplets a_1 and a_2 leading to the formation of a drop a_{12} from a Laminar Jet with $We=16.48$. **(a)** shows event before the collision where the droplet a_2 approaches a_1 , **(b)** shows the event during the incipience of contact initiated between the two droplets and **(c)** shows permanent coalescence of droplets with air-entrapment. Each of the part figures in **(a)**, **(b)** and **(c)** show **(i)** Liquid Volume fraction profile, **(ii)** Shear stress (Pa) distribution over the droplet and **(iii)** Instantaneous velocity along the axis normalized by the mean velocity at the inlet V_0 .

A liquid jet with a constant flow rate Q could present complex droplet merging dynamics downstream owing to factors such as variations in breakup length, surface oscillations, and to a degree the droplet diameters emanating from the jet. Potentially for the cases we have examined, typically higher flow rates lead to higher Weber number values causing a greater degree of non-linearity in jet behaviour and droplet breakup. One such event that is numerically resolved is shown in [Fig. 7a](#) where

droplets \mathbf{a}_2 which is prolate in shape, collides with \mathbf{a}_1 that is oblate in shape to form \mathbf{a}_{12} for a $We=16.48$. Under these circumstances, it can be seen that an air entrapment is formed during the incipience of merging tends to move towards the fore-end of the droplet \mathbf{a}_{12} from the interface curvature formed owing to merging. Interestingly, at $t^*=8.0049$, the droplet \mathbf{a}_{12} begins to exhibit a dumbbell-shaped profile, and at $t^*= 8.2102$ two droplets, \mathbf{b}_2 and \mathbf{b}_1 are formed out of \mathbf{a}_{12} . Here, one must note that the subscripts 2 and 1 associated with \mathbf{b} droplets are only used to identify that \mathbf{b}_1 is downstream to \mathbf{b}_2 but unlike the subscripts used with \mathbf{a}_1 and \mathbf{a}_2 which indicate that both the time of formation and their downstream progression. We shall term this as '*reflexive-like*' separation since the behaviour we observe is synonymous to an ideal *reflexive* separation evidenced during head-on collisions for droplets (Qian and Law, (1997); Ashgriz and Poo, (1990)) owing to its striking similarities such as i) droplets contracting inwards due to reflexive action (towards the axis) after a collision pushing the collided masses from the centre is observed, ii) the formation of dumbbell-shaped profile development after the incipience of merging as shown in Fig. 7a at $t^*= 8.0049$, iii) the formation of a cylindrical ligament as seen during $t^*= 8.2102$ (a close-up picture is detailed in Fig. 7b) and in Fig. 7c during separation and iv) merging of the cylindrical ligament at $t^*= 8.4154$ with \mathbf{b}_1 is observed in Fig. 7d, which leads to an air entrapment similar to that evidenced in Figure 20 in the published work of Ashgriz and Poo (1990).

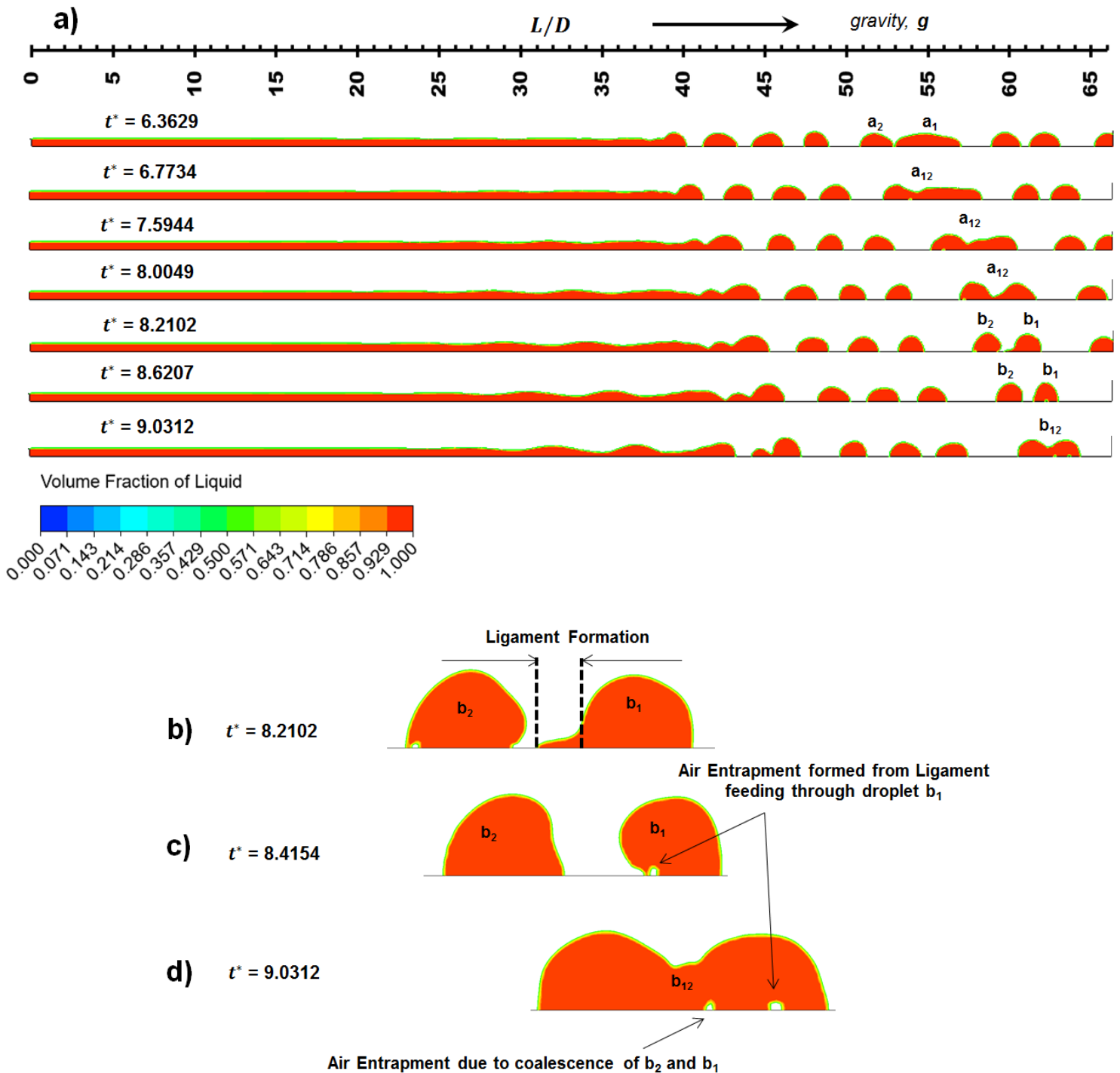


Fig.7. Liquid volume fraction is shown illustrating the merging of droplets a_1 and a_2 leading to the formation of a drop a_{12} from a Laminar Jet with $We=16.48$. The droplet formed undergoes *reflexive-like* separation to form primary droplets b_1 and b_2 ; as a minuscule temporal-event, the droplets *re-merge* to form b_{12} . A close-up of such events showing intricate details such as **b)** ligament formation during reflexive-like separation, **c)** air-entrapment created owing to a ligament that is being absorbed within droplet b_1 and **d)** *re-merge* response showing the formation of b_{12} including air-entrapment formed during merging.

We shall allude that the reflexive separation during binary droplet collisions reported previously were observed for droplet *Weber numbers* > 19 (Ashgriz and Poo, (1990)). Interestingly, this is closer to the jet Weber number ($We=16.48$) in the present case considering that primary droplets examined herein have $>1.5D$ as per Rayleigh's theory that will eventually lead to higher 'droplet Weber numbers'. Indeed from a droplet topological point of view, we shall still remark this behaviour as only '*reflexive-like*' owing to a critical difference with the ideal reflexive separation wherein a torus-like formation during merging is not observed (see Figure 4 in the published work of Ashgriz and Poo (1990)). Also, experimental observations during a head-on collision of binary droplets indicate that when a reflexive separation occurs, a shape-structured development is presented after the droplets coalesce and before they breakup. The shape of the merged droplet transforms from oblate to prolate and then changes back to oblate. In the present study, only a *partial coalescence* between drops moving downstream with surface oscillations which imprint the formation of a single oblate droplet is numerically predicted owing to which the surface reflex is not as strong as one would witness for drops approaching each other in a head-on collision. As illustrated by various researchers both experimentally (Qian and Law, (1997); Ashgriz and Poo, (1990)) and numerically (Pan and Suga, (2005)) a reflexive separation may or may not be associated with the formation of satellite drops. However, at least within the jet Weber numbers examined in this study, the formation of satellite droplets was not conclusively evident during the separation event detailed in Fig. 7.

Although markedly different from an ideal reflexive merging and separation patterns formed from binary droplet collisions that are either head-on, or that owing to off-centre and that correspond to directionally different drop motions, which have been extensively reported previously in both experimental data and from simulations, we have detailed some remarkable similarities with the way that droplets interact downstream from a liquid jet. It is important to re-emphasize that all droplet merging patterns examined in the present work are continually disintegrated from a single laminar jet and with surface oscillations moving downstream, and all collisions are purely in-tandem. Therefore, a closer examination until after the *reflexive-like* separation detailed above leads to another exciting event wherein a *re-merge* response of the droplets \mathbf{b}_2 and \mathbf{b}_1 takes place leading to the formation of \mathbf{b}_{12} as

seen in Fig. 7a; a closer image of the same is shown in Fig. 7d. Features such as the motion of the air-bubble relative to one another and to that of the droplet, the spatial and temporal variation of the air-bubble within the droplet, and their life-span are all certainly well beyond the scope of the present examination.

3.3 Merging Behaviour of Primary with Satellite Droplets and Vice-Versa

For a liquid jet with a constant flow rate Q at higher Weber numbers, under the influence of gravity, the onset of nonlinearities in the form of surface disturbances can lead to the formation of several types of satellite droplets alongside primary droplets (Chaudhary and Maxworthy, (1980)). Fig. 8 shows the liquid volume fractions that numerically evidence the formation of several types of satellite droplets with the presence of surface oscillations for $We=16.48$. As shown in Fig. 8a, the satellite droplet s_1 forward merges with the primary droplet a_1 forming the droplet s_1a_1 . In another instance, it is seen that the satellite s_1 rear merges with the primary droplet a_2 forming a_2s_1 shown by Fig. 8b. Also, simultaneous merging of two satellite droplets with a primary droplet is predicted when swellings sw_{1j} and sw_{2j} are formed in the jet. These swellings lead to the formation of satellites s_1 and s_2 that simultaneously merge with the primary drop a_1 , as seen in Fig. 8c. The current numerical results are consistent with the observations demonstrated in experimental results wherein the satellite droplets have shown the ability to merge on the foreside, the aft side and simultaneously on both sides of the primary droplet (Pimbley and Lee, (1977); Vassallo and Ashgriz, (1991)). However, to the best of author's knowledge, a numerical prediction of a forward, rear and simultaneous merging of droplets from a liquid jet is being reported for the first time within the current effort.

Additionally, the breakup of the swelling sw_{2j} , which is closer to the liquid core produces a primary drop a_2 and a satellite drop s_3 . Interestingly, the satellite s_3 although formed on the aft side of the droplet a_2 may be anticipated to rear merge with a_2 . Instead, the satellite s_3 is absorbed by the moving jet liquid core, denying the event of s_3 merging with a_2 . This unique merging behaviour of satellites with the jet liquid core has not been previously reported to the best of author's knowledge and is, therefore, a proposition to future experimental investigation. In each of the cases shown in Fig.8 (a-c), we note that the merging of satellites with the primary droplets and with the jet liquid core demonstrates the presence of an air entrapment that is

quite diminutive in comparison to the air entrapment formed from primary droplet collisions that are shown in Fig. 7.

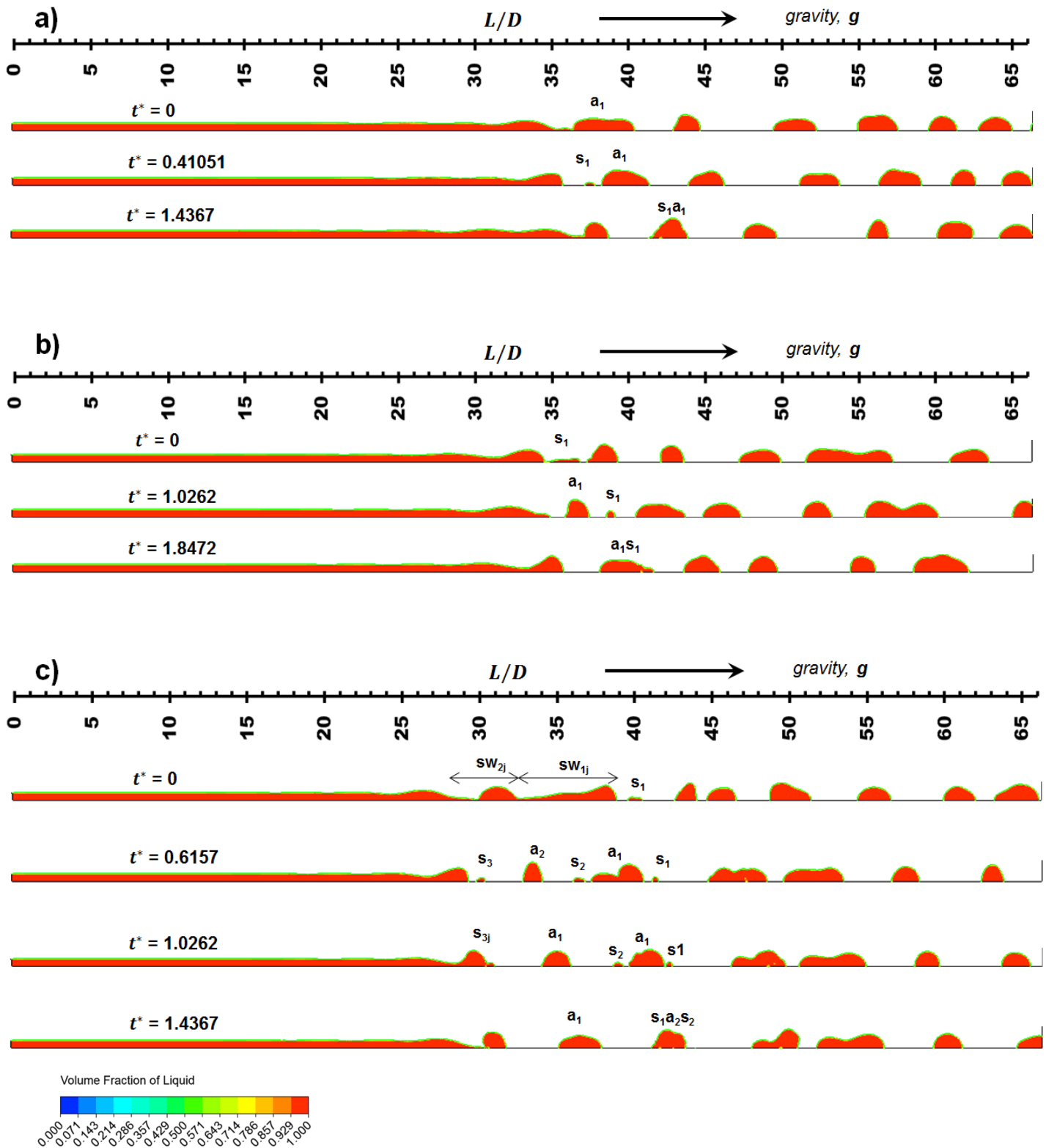


Fig.8. Liquid volume fraction profiles showing **a)** forward merging, **b)** rear merging and **c)** simultaneous merging of satellite droplets emanated from a liquid jet with $We=16.48$. The formation of satellite s_3 from swelling sw_{2j} merging back to the moving liquid jet core is seen in the part figure c).

We highlight that unlike a controlled jet breakup, for example, by means of velocity modulation or jet vibration an '*infinite-satellite condition*' may prevail wherein the velocities of satellite drops can match with the primary droplets as observed from the works of Pimbley and Lee (1977) and Vassallo and Ashgriz (1991) which may lead to satellites exiting the domain outlet without coming into contact with primary drop(s). However, within the scope of the present simulations using a fixed Q value, wherein breakup is dominated by spatially growing disturbances with composition of many wavelengths, we observe that unlike primary droplets, all satellite droplets that were formed eventually merge with either the primary droplets or with the jet liquid core as a particular case and an *infinite-satellite condition* was not observed.

4 Conclusions

In this paper, we have detailed specific merging responses of primary and satellite droplets that disintegrate from laminar Newtonian liquid jet using numerical simulations. Developing from the previously published methodology of Viswanathan (2019) that uses the VOF approach alongside the Continuum Surface Force representation to modelling laminar liquid jets, in the current effort, a sanity check was first performed against the Laplace-Young equation for assessing the numerical accuracy of the pressure jump across the disintegrated droplet interface. For the range of droplet sizes that were examined in this study, the average relative error between the numerical model and theoretical description was $\sim 5.7\%$, suggesting that the parasitic currents are negligible across the interface. Our numerical findings demonstrate the following droplet merging characteristics emanated from liquid jets:

- (i) For primary droplet disintegrations, the surface oscillations tend to aid collision of droplets that can lead to a *permanent coalescence* forming a single drop with no further breakup until it reaches the target downstream. With an increase in flow rate, more complex dynamics is presented where primary droplets partially coalesce and exhibit *reflexive-like separation* due to the presence of undamped surface oscillations in the droplet that is formed and further show *re-merge* characteristics forming a single droplet with no further breakup. The *reflexive-like* separation in droplets observed from the liquid jet disintegrations shows remarkably similar features that were

experimentally revealed by several researchers (Ashgriz and Poo, (1990); Qian and Law, (1997); Orme, (1997); Munnannur and Reitz, (2007); Krishnan and Loth, (2015) for binary droplet collisions but then show critical topological differences when merging begins prior to the separation event.

(ii) When satellite drops are produced, they exhibit surface oscillations as well, and tend to merge on the aft side, the foreside and sometimes simultaneously merge on both sides of a primary droplet that are present downstream. This result is consistent with those observed experimentally by Pimbley and Lee (1977) and Vassallo and Ashgriz (1991). Besides, our results show a new merging pattern where the satellite droplet that is formed can merge back into the moving jet liquid core rather than merging with the primary droplet that may be present downstream.

(iii) An air bubble in the form of air-entrapment is numerically predicted within the formed drop regardless of whether a primary or a satellite droplet coalesces with another primary droplet. The formation of an air-bubble is also evidenced when a satellite droplet merges with the moving liquid core.

Although we have presented some unique features that augment the understanding of the intricate characteristics of droplet merging using VOF technique, however, our results do not show features wherein (i) a satellite never merges with a primary droplet but reaches the target without encountering any collision and (ii) cases where bouncing behaviour of droplets are featured from liquid jets (Suñol and Cinca, 2015). The responses presented in this study such as the satellite droplet merging with the jet liquid core and a *reflexive-like* separation of primary droplets have not been reported before to the best of author's knowledge, and hence, we recommend experimental endorsements as an outcome of this study.

Acknowledgements

The author wishes to thank Mr Steven Brandon and Mr Alex Webster for managing the computing resources and HPC support.

This work was supported by ANSYS Academic Research Partnership Grant.

References

1. Ashgriz, N., Poo, J.Y., 1990. Coalescence and separation in binary collision of liquid drops. *J. Fluid. Mech.* 221, 183–204.
2. Becker, E., Hiller, W.J., Kowalewski, T.A., 1991. Experimental and theoretical investigation of large-amplitude oscillations of liquid droplets. *J. Fluid Mech.* 231, 189–210.
3. Borthakur, M.P., Biswas, G., Bandyopadhyay, D., 2017. Formation of liquid drops at an orifice and dynamics of pinch-off in liquid jets. *Phys. Rev. E.* 96, 013115.
4. Brackbill. J., Kothe D., Zemach, C., 1992. A continuum method for modeling surface tension. *J. Comput. Phys.* 100, 335–354.
5. Brazier-Smith, P.R., Jennings, S.G., Latham, J., 1972. The interaction of falling water drops: coalescence, *Proc. R. Soc. Lond. A* 326, 393-408.
6. Chandrasekhar, S., 1961. *Hydrodynamic and Hydromagnetic Stability*. Oxford University Press, Oxford (Chapter XII).
7. Chakraborty, I., Rubio-Rubio, M., Sevilla, A., Gordillo, J.M., 2016. Numerical simulation of axisymmetric drop formation using a coupled level set and volume of fluid method. *Int. J. Multiphase Flow* 84, 54–65.
8. Chaudhary, K.C., Maxworthy, T., 1980. The nonlinear capillary instability of a liquid jet. Part 3. Experiments on satellite drop formation and control. *J. Fluid Mech.* 96 (2), 287–297.
9. Clanet, C., Lasheras, J.C., 1999. Transition from dripping to jetting. *J. Fluid Mech.* 383, 307–326.
10. Delteil, J., Vincent, S., Erriguible, A., Subra-Paternault, P., 2011. Numerical investigations in Rayleigh breakup of round liquid jets with VOF method. *Comput. Fluids* 50, 10–23.
11. Driessen, T., Sleutel, P., Dijksman, F., Jeurissen, R., Lohse, D., 2014. Control of jet breakup by a superposition of two Rayleigh–Plateau-unstable modes. *J. Fluid Mech* 749, 275–296.
12. Eggers, J., Dupont, T.F., 1994. Drop formation in a one-dimensional approximation of the Navier–Stokes equation. *J. Fluid Mech.* 262, 205–221.
13. Garc'ia, F.J., Castellanos, A., 1994. One-dimensional models for slender axisymmetric viscous liquid jets. *Phys. Fluids* 6 (8), 2676–2689.

14. Goedde, E.F., Yuen, M.C., 1970. Experiments on liquid jet instability. *J. Fluid Mech.* 40 (3), 495–511.
15. Hirt, C.W., Nichols, B.D., 1981. Volume of fluid (VOF) method for the dynamics of free boundaries. *J. Comput. Phys.* 39, 201–225.
16. Krishnan, K., Loth, E., 2015. Effects of gas and droplet characteristics on drop-drop collision outcome regimes. *Int. J. Multiphase Flow*, 77, 171–186.
17. Lieb, S.J., Goldstein, M.E., 1986. Generation of capillary instabilities on a liquid jet. *J. Fluid Mech.* 168, 479–500.
18. Mashayek, F., Ashgriz, N., Minkowycz, W.J., Shotorban, B., 2003. Coalescence collision of liquid drops, *Int. J. Heat Mass Transfer.* 46 (1) 77–89.
19. Moallemi, N., Li, R., Mehravaran, K., 2016. Breakup of capillary jets with different disturbances. *Phys. Fluids* 28, 012101.
20. Munnannur, A., Reitz, R.D., 2007. A new predictive model for fragmenting and non-fragmenting binary droplet collisions. *Int. J. Multiphase Flow*, 33, 873–896.
21. Nayfeh, H., 1970. Nonlinear stability of a liquid jet. *Phys. Fluids* 13, 841–847.
22. Nikolopoulos, N., Bergeles, G., 2011. The effect of gas and liquid properties and droplet size ratio on the central collision between two unequal-size droplets in the reflexive regime. *Int. J. Heat Mass Transfer* 54, 678–691.
23. Orme, M., 1997. Experiments on droplet collisions, bounce, coalescence and disruption, *Prog. Energy Combust. Sci.* 23 (1), 65–79.
24. Pan, Y., Suga, K., 2005. Numerical simulation of binary liquid droplet collision. *Phys. Fluids* 17, 082105.
25. Pan, Y., Suga, K., 2006. A numerical study on the breakup process of laminar liquid jets into a gas. *Phys. Fluids* 18, 0521011.
26. Pimbley, W.T., Lee, H.C., 1977. Satellite droplet formation in a liquid jet. *IBM J. Res. Dev.* 21, 21–30.
27. Plateau, J., 1873. *Statique expérimentale et théorique des liquides soumis aux seules forces moléculaires* (Gauthier-Villars, Trubner et cie, Paris).
28. Premnath, K.N., Abraham, J., 2005. Simulations of binary drop collisions with a multiple-relaxation-time lattice-Boltzmann model, *Phys. Fluids.* 17 (12), 122105.
29. Qian, J., Law, C.K., 1997. Regimes of coalescence and separation in droplet collision, *J. Fluid. Mech.* 331, 59–80.
30. Rayleigh, L., 1878. On the instability of jets. *Proc. Lond. Math. Soc.* 10, 4-13.

31. Rayleigh, L., 1882. Further observations upon liquid jets. *Proc. Lond. Math. Soc.*, 34, 130–145.
32. Rivero-Rodríguez, J., Pérez-Saborid, M., 2017. An efficient finite volume method for one-dimensional problems with application to the dynamics of capillary jets. *Comput. Fluids* 154, 1, 132–141.
33. Rutland, E., Jameson, J., 1970. Theoretical prediction of the sizes of droplets formed in the breakup of capillary jets. *Chem. Eng. Sci.* 25, 1689–1698.
34. Sallam, K.A., Dai, Z., Faeth, G.M., 2002. Liquid breakup at the surface of turbulent round liquid jets in still gases. *Int. J. Multiphase Flow*, 28, 427–449.
35. Sauter, U., Buggisch, H., 2005. Stability of initially slow viscous jets driven by gravity. *J. Fluid Mech.*, 533, 237-257.
36. Savart, F., 1833. Mémoire sur la constitution des veines liquides lancées par des orifices circulaires en mince paroi. *Ann. de Chim.* 53, 337–386.
37. Suñol., F., González-Cinca, R., 2015. Liquid jet breakup and subsequent droplet dynamics under normal gravity and in microgravity conditions. *Phys. Fluids* 27 (7), 077102.
38. Tomotika, S., 1935. On the instability of a cylindrical thread of a viscous liquid surrounded by another viscous liquid. *Proc. Roy. Soc. Lond. A* 150, 322–337.
39. Vassallo, O.P., Ashgriz, N., 1991. Satellite formation and merging in liquid jet breakup. *Proc. R. Soc. Lond. A* 433, 269–286.
40. Viswanathan, H., 2019. Breakup and coalescence of drops during transition from dripping to jetting in a Newtonian fluid. *Int. J. Multiphase Flow*, 112, 269–285.
41. Xiao, F., Dianat, M., McQuirk, J.J., 2016. A robust interface method for drop formation and breakup simulation at high density ratio using an extrapolated liquid velocity. *Comput. Fluids* 136, 402–420.
42. Xie, L., Yang, Li-jun., Ye, Han-yu., 2017. Instability of gas-surrounded Rayleigh viscous jets: Weakly nonlinear analysis and numerical simulation. *Phys. Fluids* 29 (7), 074101.
43. Youngs, D., 1982. Time-dependent multimaterial flow with large fluid distortion. In: Morton, K.W., Baibes, M.J. (Eds.), *Numerical Methods for Fluid Dynamics*, pp. 273–285.
44. Yuen, M.C., 1968. Non-linear capillary instability of a liquid jet. *J. Fluid Mech.* 33, 151–163.